04,16

Luminescence properties of $Yb_{1-x}Sc_xPO_4$ solid solutions

© D.A. Spassky[1,2], I.V. Nikiforov[3], A.N. Vasil'ev[1]

[1] Skobeltsyn Institute of Nuclear Physics, Moscow State University, Moscow, Russia
[2] Institute of Physics, University of Tartu, Tartu, Estonia
[3] Moscow State University, Moscow, Russia

E-mail: spas@srd.sinp.msu.ru

Received November 24, 2023
Revised December 4, 2023
Accepted December 5, 2023

Luminescence properties of $Yb_{1-x}Sc_xPO_4$ solid solutions obtained by solid-state reaction were studied. According to the data of XRD analysis the synthesized solid solutions are single phase; the change of crystal lattice parameters is described by Vegard's law. The origin of emission centers was determined under the excitation in UV and VUV spectral regions. It was shown that all solid solutions are characterized by the emission in UV region related to the charge transfer luminescence ($x \neq 1$) or radiative relaxation of excitons ($x = 1$). The increased efficiency of energy transfer to the emission centers was shown for solid solutions and attributed to the separation length constrain of the non-thermalized electrons and holes. This effect results in the UV luminescence enhancement in $Yb_{1-x}Sc_xPO_4$ solid solutions and may be of applied interest for the creation of new phosphors with intense luminescence in the UV range.

Keywords: energy transfer, UV-luminescence, charge transfer luminescence, solid solutions, $ScPO_4$, $YbPO_4$.

DOI: 10.21883/0000000000

1. Introduction

Phosphors with ultraviolet (UV) luminescence are of interest for high energy physics, medicine, environment, security applications [1–4]. UV-emitting scintillation detectors allow solar-blind radiation detectors to be used and, thus, to solve the ambient illumination problem [1]. 200–260 nm UV emission has antibacterial properties and may be used for surface sterilization, in water treatment systems and surgery [5,6]. In addition, UV phosphors, including long-persistence phosphors, may be used in solar panels and in photocatalysis [7,8].

It has been shown before that wide-gap phosphates with structural type of monazite and xenotime, doped with rare-earth ions Ce^{3+}, Pr^{3+} and Yb^{3+} and with ions Bi^{3+} have bright UV-luminescence [9–12]. In addition, the benefit of phosphates is in relatively low synthesis temperature, chemical stability and radiation resistance [13–15]. Luminescent properties of phosphate-based solid solutions are also widely studied [16–21]. In some cases, it was reported that solid solutions may have quantum yield higher than that of their constituents [18,21]. Improved properties are associated with the possibility of creating local nanometer-scale regions (clusters) in solid solutions where the content of one type of substitutional atoms exceeds their statistical distribution in the solution. This results in a decrease in the electron-hole pair scatter length at high-energy excitation, in increase of probability of energy transfer to luminescence centers and in the improvement of excitation localization on luminescence center [18,22,23].

As far as we know, luminescent properties of $Yb_{1-x}Sc_xPO_4$ solid solutions have not been studied before. Solid solutions constituents, $ScPO_4$ and $YbPO_4$ have UV-luminescence, however, luminescence centers of these compounds are of different origin. Thus, $ScPO_4$ features a luminescence band with a peak at 210 nm. This band is associated with radiative relaxation of self-trapped excitons with electron component localization on 3d Sc states [18,24]. Investigations of Yb^{3+}-doped phosphates have shown that, besides the IR luminescence typical for $^7F_{5/2}-{}^7F_{7/2}$ intracenter transitions in Yb^{3+}, two broad UV and blue emission bands are also observed and represent charge-transfer luminescence (CTL) [10,25,26]. CTL is a process inverse to charge transfer absorption [27,28]. For charge-transfer absorption, an electron goes from ligands to a rare-earth ion forming a charge-transfer excited state consisting of Yb^{2+} and hole delocalized on ligands that surround the ion. Charge-transfer luminescence is a radiative relaxation of this state. In this case, there are usually two bands separated by 10000 cm^{-1} which corresponds to the energy gap between $^7F_{7/2}-{}^7F_{5/2}$ levels in Yb^{3+}. CTL also features short decay times $\sim 10^{-9}-10^{-7}$ s under high-energy excitation allowing this type of luminescence to be considered for scintillation detector applications [29,30].

Luminescent properties of $Yb_{1-x}Sc_xPO_4$ solid solutions were studied herein. The study is focused on the dependence of structural and luminescent properties on solid solution composition and on competition between the UV-luminescence centers of different origin.

2. Experimental procedure

Synthesis of $Yb_{1-x}Sc_xPO_4$ solid solutions ($x = 0$, 0.01, 0.05, 0.1, 0.2, 0.4, 0.5, 0.6, 0.8, 1) was conducted by a standard solid phase method using stoichiometric amounts of Yb_2O_3 (99.99%), Sc_2O_3 (99.99%) and $NH_4H_2PO_4$ (99.99%). Initial weighed portions were homogenized in an agate mortar. The resulting solution was slowly heated up to 1490°C during 10 h, and then annealed during 50 h in air in an alundum crucible.

X-ray patterns were recorded for powder samples using Thermo ARL X'TRA diffractometer under Cu$K\alpha$-emission, $\lambda = 1.5418$ Å, in Bragg–Brentano geometry. A Peltier-cooled CCD detector was used for recording. X-ray patterns were measured at room temperature in the 2θ angle range from 15° to 70° with a step interval of 0.02°. Lattice cell parameters were measured by the Le Bail method using JANA2006 sotware. X-ray images of the prepared samples were analyzed using ICDD PDF-4 database.

The ultraviolet (UV) and vacuum-ultraviolet (VUV) luminescence and luminescence excitation spectra were measured using a specialized setup for solid-state luminescence spectroscopy. Hamamatsu L11798 deuterium discharge lamp with MgF_2 window was used as a source of excitation. The excitation wavelength was chosen using McPherson 234/302 vacuum monochromator with a dispersion of 4 nm/mm. The samples were placed into ARS vacuum cryostat designed for measurements in the range of 5–350 K, however, all measurements were performed herein at room temperature $T = 300$ K. Luminescence signal was recorded using a Shamrock 303i monochromator equipped with Hamamatsu H8259-02 counting head and Newton DU970P-BVF CCD detector. The luminescence spectra were corrected for the spectral sensitivity function of the recording system.

3. Results and discussion

3.1. X-ray diffraction analysis of $Yb_{1-x}Sc_xPO_4$ solid solutions

Figure 1 shows the X-ray patterns of the synthesized samples. Positions and number of reflexes on the X-ray patterns of obtained scandium-ytterbium phosphates match pure $ScPO_4$ (PDF Card No. 00-048-0477) and $YbPO_4$ (PDF Card No. 00-045-0530) from ICDD PDF-4 database. The absence of impurity reflexes suggest formation of a continuous solid solution series. The X-ray patterns of the phosphate solid solutions demonstrate gradual shift of the reflexes towards large angles as ytterbium is substituted by scandium. The shift towards high values of 2θ is observed for all reflexes, Figure 2 shows the reflex(0 2 0) for solid solution composition as an example. The calculation of the lattice cell parameters (Figure 3) shows their gradual decrease with increase of x, which may be described by a linear function. The resulting dependence is associated with substitution of large-radius ($r_{VII} = 0.98$ Å) Yb^{3+} by smaller Sc^{3+} ($r_{VII} = 0.87$ Å) [31]. The observed linear change of the cell parameters shows that Vegard's law is obeyed for these solid solutions [32], and the prepared solid solutions form a continuous series. Thus, the X-ray diffraction analysis has found that all synthesized samples of the solid solution series are single-phase and crystallize in the structural type of xenotime with tetragonal crystal system and space group $I4_1/amd$ (No 141).

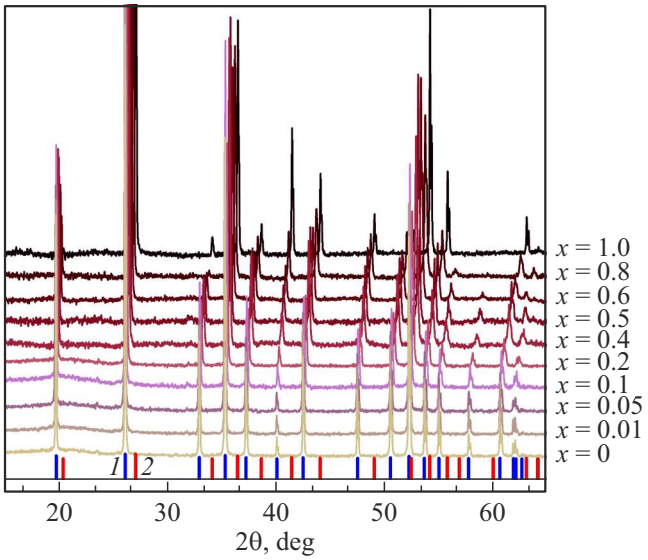

Figure 1. The X-ray patterns of $Yb_{1-x}Sc_xPO_4$ solid solution series ($x = 0$, 0.01, 0.05, 0.1, 0.2, 0.4, 0.5, 0.6, 0.8, 1) and position of Bragg reflexes for $YbPO_4$ (ICDD PDF-4 No. 00-045-0530) (*1*) and $ScPO_4$ (ICDD PDF-4 No. 00-048-0477) (*2*).

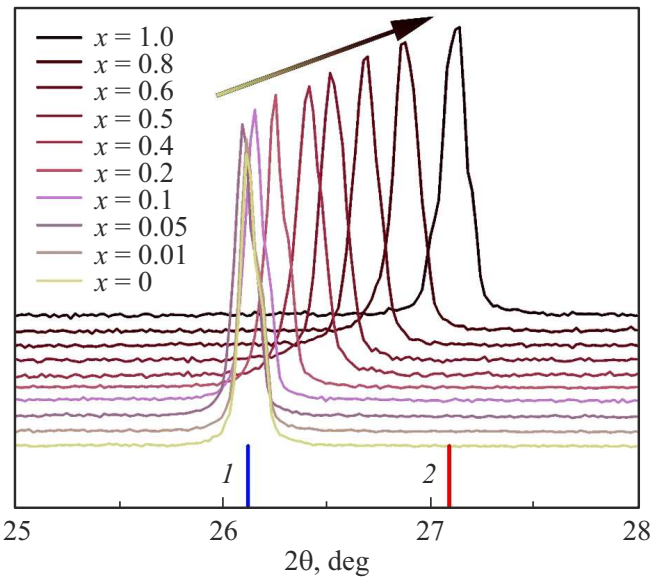

Figure 2. The main reflex position (0 2 0) for $Yb_{1-x}Sc_xPO_4$ solid solution ($x = 0$, 0.01, 0.05, 0.1, 0.2, 0.4, 0.5, 0.6, 0.8, 1), and position of this reflex for $YbPO_4$ (ICDD PDF-4 No. 00-045-0530) (*1*) and $ScPO_4$ (ICDD PDF-4 No. 00-048-0477) (*2*).

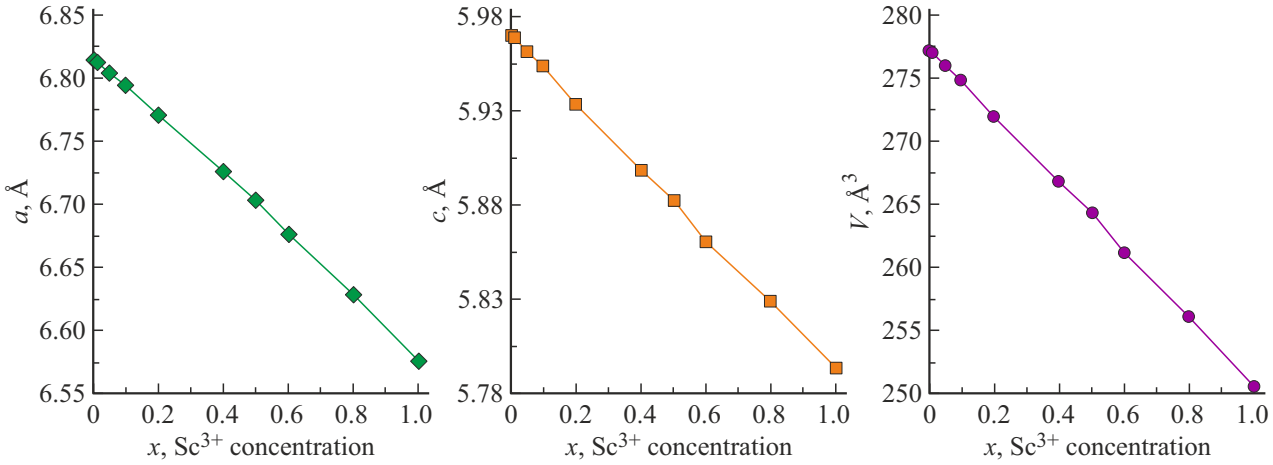

Figure 3. The lattice parameters a, c and the lattice volume for $Yb_{1-x}Sc_xPO_4$ solid solution ($x = 0$, 0.01, 0.05, 0.1, 0.2, 0.4, 0.5, 0.6, 0.8, 1).

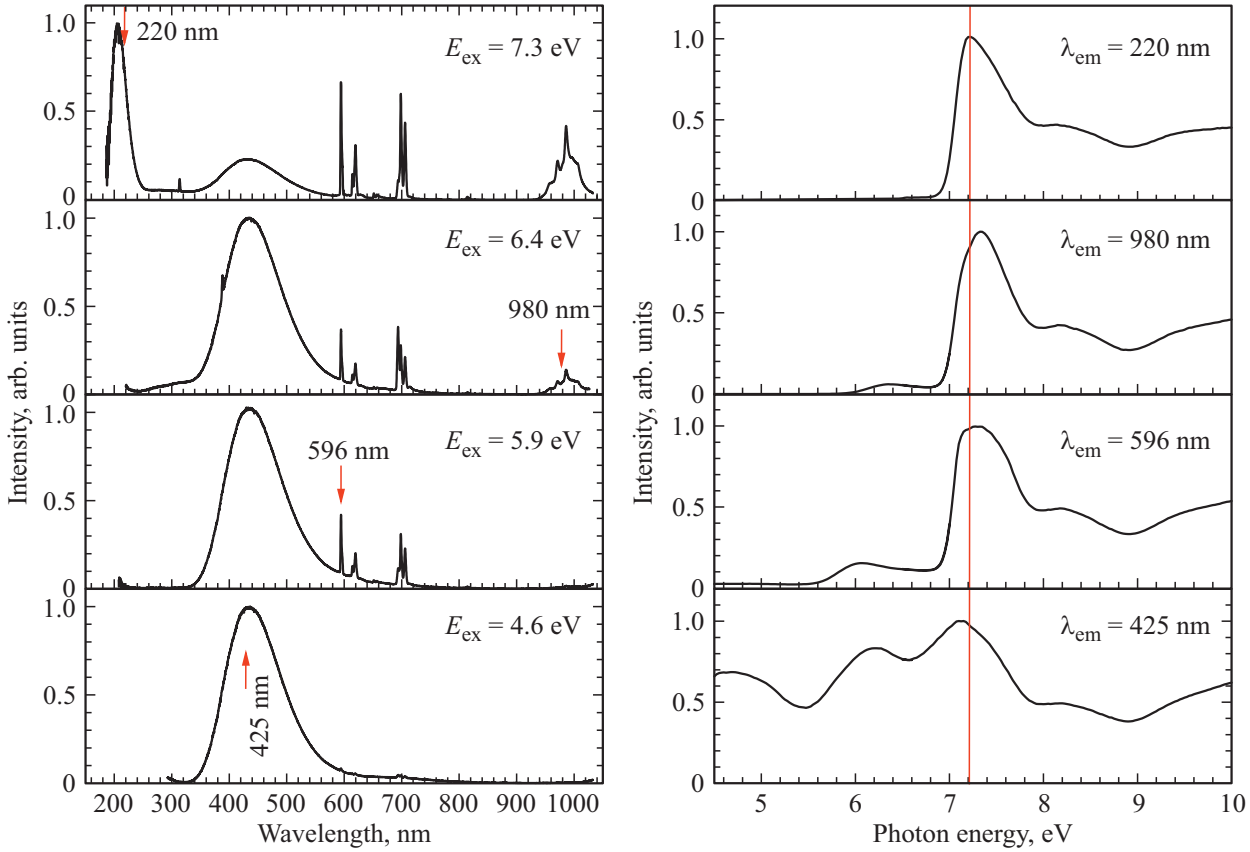

Figure 4. The luminescence (left) and the luminescence excitation (right) spectra for $ScPO_4$. Excitation energy for luminescence spectra and excitation spectra recording wavelength are shown in the figures. The red vertical line in the right figure marks the exciton peak position.

3.2. Luminescent properties of $Yb_{1-x}Sc_xPO_4$ solid solutions

The luminescence spectra measured at different excitation energies for the final composition with $x = 1$ ($ScPO_4$) are shown in Figure 4. The luminescence spectrum measured at the excitation energy of 7.3 eV corresponding to interband transitions has two wide bands with peaks at 210 nm and 425 nm, and a set of narrow bands. According to [18,24], the luminescence band at 210 nm is the inherent band for $ScPO_4$ and is caused by the radiative relaxation of self-trapped excitons with an electron component localized

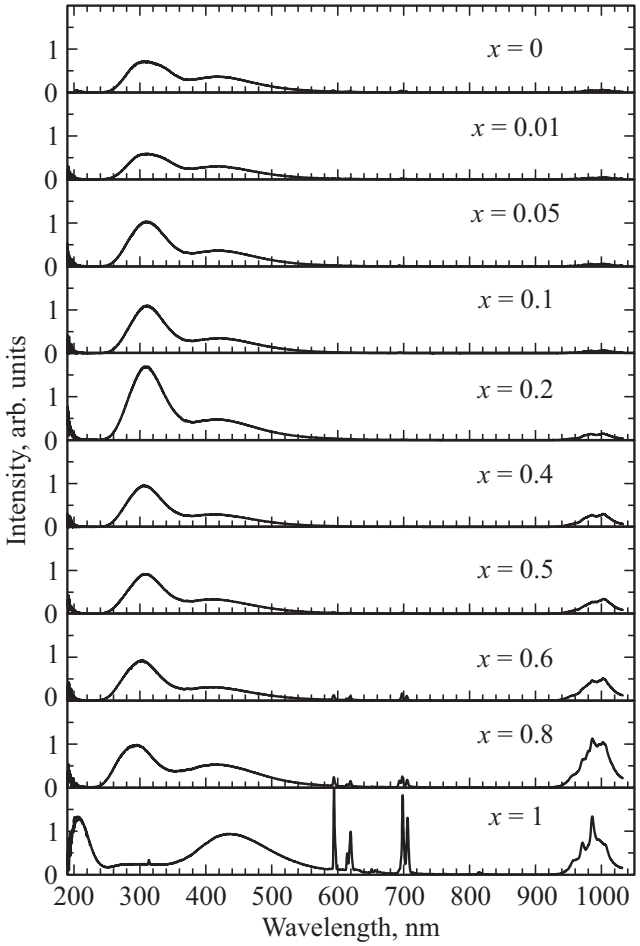

Figure 5. The luminescence spectra of $Yb_{1-x}Sc_xPO_4$ series at $E_{ex} = 9$ eV.

on 3d Sc states and with a hole component localized on 2p O states. This band is excited from the fundamental absorption edge region, the first excitation peak is observed at 7.2 eV (Figure 4) and is due to direct creation of excitons [33]. The wide band excitation spectrum at 425 nm has a set of bands in the crystal transparency region, thus, this band may be assigned to the luminescence centers associated with crystalline structure defects. Selective excitation of this band is possible in the low-energy peak at 4.6 eV. Narrow bands are observed in the 310, 580–720 and 950–1050 nm region and are attributed to the presence of uncontrolled Gd^{3+}, Eu^{3+} and Yb^{3+} impurities, respectively. The luminescence excitation spectra for Eu^{3+} and Yb^{3+} luminescence bands have low-intensity wide bands below the fundamental absorption edge with peaks at 6.03 (Eu^{3+}) and 6.41 (Yb^{3+}) eV. These bands are attributed to charge-transfer transitions and the difference of 0.38 eV between the excitation band peaks of Eu^{3+} and Yb^{3+} agrees well with 0.43 eV predicted within the chemical shift model developed by Dorenbos [34].

Luminescence spectra of the whole sample series at the excitation energy of 9 eV are shown in Figure 5. Except for the finished composition with $x = 1$ ($ScPO_4$), the spectra have two bands with peaks in UV (290–310 nm) and blue (420–430 nm) spectral regions and a group of IR-region bands (950–1050 nm). The observed luminescence bands are attributed to intracenter transitions $^7F_{7/2}-^7F_{5/2}$ in Yb^{3+}. Wide UV and blue spectral bands may be assigned to CTL, the difference between the band peaks is $\sim 9800\,cm^{-1}$, which agrees well with the energy gap between $^7F_{7/2}-^7F_{5/2}$ levels in Yb^{3+} — $10000\,cm^{-1}$ [27,28]. It should be noted that the solid solutions do not have any exciton luminescence band typical for $ScPO_4$. For instance, in $Y_{1-x}Sc_xPO_4$ solid solutions, this band was observed up to low concentrations of scandium ($x = 0.01$), and the band intensity achieved its peak at $x = 0.5$ [35]. It may be suggested that occurrence of charge-transfer states in $Yb_{1-x}Sc_xPO_4$ ($x \neq 1$) with participation of ytterbium electron states results in quenching of the exciton luminescence.

Relative intensity of IR luminescence and CTL depends on the solid solution composition (Figure 6). IR band intensity gradually decreases with an increase in ytterbium concentration in the solution. Such dependence is attributed to concentration quenching of 4f–4f luminescence. Actually, the distance at which excitation may migrate over the ytterbium sublattice increases with ytterbium concentration which, in turn, increases the probability to be captured by a defect and reduces the probability of radiative relaxation of excitation. CTL intensity non-monotonously depends on the scandium content. Intensity increases with an increase in Sc^{3+} concentration and achieves its peak at $x = 0.2$ exceeding the CTL intensity in $YbPO_4$ by more than 2 times. With the increase of Sc^{3+} content up to 0.4, the intensity becomes 1.7 times lower and with further increase has a low dependence on composition. An increase in the luminescence intensity has been observed earlier in various solid solutions both for impurity and

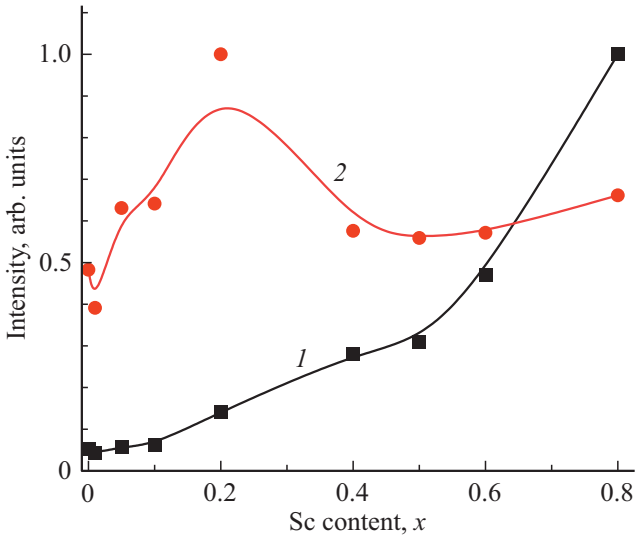

Figure 6. The relative intensities of IR luminescence (*1*) and charge-transfer UV-luminescence (*2*) derived from the luminescence spectra shown in Figure 5.

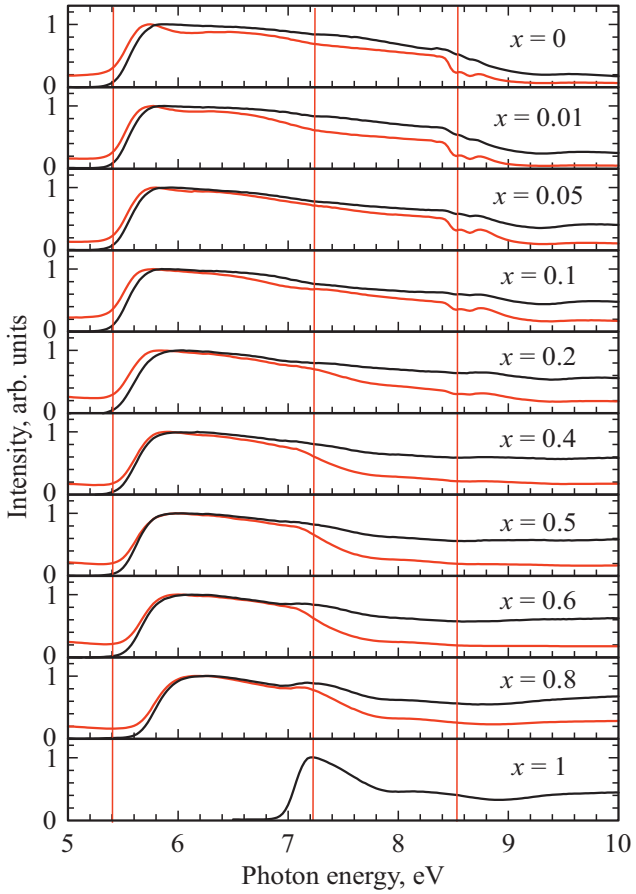

Figure 7. Luminescence excitation spectra of $Yb_{1-x}Sc_xPO_4$ series, $\lambda_{lum} = 970$ nm (red curves) and 290 nm (black curves) for all samples, except for $ScPO_4$, where $\lambda_{lum} = 220$ nm. Solid vertical line at 5.4 eV corresponds to low-energy threshold of the charge-transfer band for $YbPO_4$, line at 7.2 V corresponds to the exciton peak energy position in $ScPO_4$, line at 8.73 eV corresponds to the exciton peak position in $YbPO_4$.

intrinsic luminescence [36–39]. Increase of intensity in solid solutions is attributed to the limitation of path length for separated electron-hole pairs during thermalization and migration. This will increase the probability of exciton formation or trapping of geminate electrons and holes by the same emission center. It is suggested that the observed dependence for CTL is attributed to the limitation of electron and hole path length in $Yb_{1-x}Sc_xPO_4$.

CTL and IR luminescence excitation spectra ($x \neq 1$) as well as exciton luminescence spectra ($x = 1$) are shown in Figure 7. Peak at 7.2 eV that is attributed to exciton formation at 2p O−3d Sc transition in $ScPO_4$ is also revealed in the excitation spectra of solid solutions with high scandium content ($x = 0.8,\ 0.6$). This peak shows that the energy of such excitons is transferred to the CTL and IR luminescence centers resulting in a total absence of luminescence of self-trapped scandium excitons.

The low-energy threshold in the excitation spectra shifts intermittently into the low energy region to 5.6 eV ($x = 0.8$) and then gradually to 5.4 eV with further decrease in scandium content in the solid solution. Low-energy threshold shift in the spectra is attributed to the possibility of CTL and IR luminescence excitation through the charge-transfer band. The threshold is revealed in the luminescence excitation spectrum at the energies at which the exciting radiation becomes totally absorbed by the sample, i.e. in the region when the light penetration depth of the sample becomes approximately equal to the sample thickness. The absorption coefficient in the charge-transfer band grows proportionally to the ytterbium concentration $(1 - x)$. On the assumption of the Gaussian shape of this absorption coefficient for ytterbium concentrations > 20%, this threshold will correspond to the long-wavelength band edge and will move with concentration growth into the low-energy region, and its slope will increase. Due to high ytterbium concentration, excitation reaches saturation in the region much wider than full width at half maximum of the absorption band of a single ytterbium ion.

The band gap behavior with the change of solid solution composition from $ScPO_4$ to $YbPO_4$ is important for the analysis of the luminescence excitation spectra. As far as we know, the experimental data on $YbPO_4$ band gap is not available in literature.

$YbPO_4$ band structure was calculated within the density functional theory in [40]. According to the calculation, $E_g(YbPO_4) = 6.13$ eV and defined by direct electronic transitions in point Γ of the Brillouin zone. Moreover, the valence band top is formed by mixing 2p O and 3p P states with low contribution from 3s P and 4f Yb states, and the conduction band bottom is formed by 5d Yb states with minor contribution of 3p P states. $ScPO_4$ band structure was calculated in various approximations within the density functional theory in several papers [41–43]. Depending on the applied approximation, E_g varies in the range of 4.11−4.6 eV and is defined by electronic transitions from 2p O and 3p P to 3d states of Sc that form the conduction band bottom. Thus, the band structure calculations suggest that E_g $(ScPO_4) < E_g$ $(YbPO_4)$. However, it shall be taken into account that band structure calculations usually result in underestimation of the crystal band gap. Thus, the experiments for $ScPO_4$ have shown that the band gap is 7.2−7.6 eV [24,44], which is by ∼ 3 eV higher than the calculated values.

The band gap of $YbPO_4$ and solid solutions with high ytterbium content may be estimated from the IR luminescence excitation spectra analysis. A fine structure consisting of narrow peaks at 8.57 and 8.73 eV is observed in the spectra. It has been found earlier for $LiY_{1-x}Yb_xP_4O_{12}$ solid solutions that the similar fine structure in CTL excitation spectra is attributed to the energy transfer from self-trapped excitons and excitons localized near defects [45]. The same origin of narrow peaks may be suggested in $Yb_{1-x}Sc_xPO_4$ excitation spectra. Thus, the peak at 8.57 eV may be due to formation of excitons localized near defects and the peak at 8.73 eV may be due to formation of excitons that are then self-trapped. The high-energy peak position at 8.73 eV

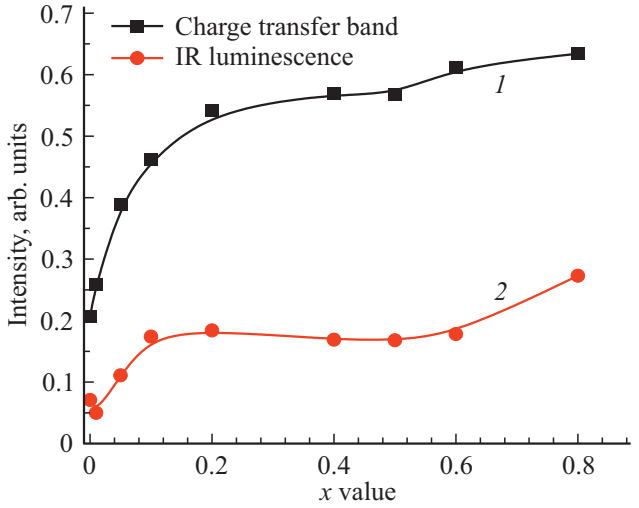

Figure 8. Dependence of the relation of the intensity at $E_{ex} = 9$ eV and intensity on the first excitation peak $E_{ex} = 5.6-6.1$ eV in excitation spectra (Figure 7) on the solid solution composition for CTL (curve *1*) and IR luminescence (curve *2*).

may be used to estimate the band gap in $YbPO_4$. This value is by approximately 2.6 eV higher than that obtained in the DFT calculation [40], which corresponds to the above mentioned band gap underestimation in this calculation method for $ScPO_4$.

In the CTL excitation spectra, the intensity only slightly decreases in the energy region above the band gap compared with the intensity in the charge-transfer bands. It should be noted that, in previously investigated garnets and aluminates, the excitation intensity decreased considerably when the excitation energy exceeded the band gap [46,47]. The studied $Yb_{1-x}Sc_xPO_4$ solid solutions feature efficient energy transfer of separated electron-hole pairs to the CTL luminescence centers. Moreover, the radiative relaxation efficiency of electrons and holes in interband excitation increases for solid solutions with intermediate values of x (Figure 8). This is an additional argument in favor of the assumption that the e-h pairs path length in this solid solution series is limited during thermalization and further migration over the crystal to the luminescence centers. Thus, the investigated solid solutions may be of interest for application as converters of high-energy radiation into UV and blue luminescence.

4. Conclusion

Using the solid-phase synthesis method, the $Yb_{1-x}Sc_xPO_4$ ($x = 0$, 0.01, 0.05, 0.1, 0.2, 0.4, 0.5, 0.6, 0.8, 1) solid solution series has been obtained. Interpretation of the X-ray patterns has shown that formation of a continuous solid solution series took place. The lattice parameters a, c and the lattice cell volume decrease linearly with ytterbium substitution by scandium in accordance with Vegard's law. It is shown that exciton luminescence is observed only in the luminescence spectra for the $ScPO_4$ while, energy transfer from excitons to charge-transfer states occurs in solid solutions. CTL intensity depends on the solid solution composition and is maximal at $x = 0.2$. The excitation spectra analysis suggests that the increase in intensity is attributed to the limitation of electron-hole pair path length in solid solutions. The band gap of $YbPO_4$ was also estimated by means of the excitation spectra analysis as 8.73 eV. It has been concluded that $Yb_{1-x}Sc_xPO_4$ solid solutions may be of interest for applications as UV phosphors with high luminescence yield.

Funding

The research was supported by grant No. 21-12-00219 of the Russian Science Foundation Enhancement of energy conversion efficiency in luminescent and scintillating materials based on solid solutions and composites.

Conflict of interest

The authors declare that they have no conflict of interest.

References

[1] D. Welch, M. Buonanno, V. Grilj, I. Shuryak, C. Crickmore, A.W. Bigelow, G. Randers-Pehrson, G.W. Johnson, David J. Brenner. Sci. Rep. **8**, 2752 (2018). https://doi.org/10.1038/s41598-018-21058-w
[2] Xianli Wang, Yafei Chen, Feng Liu, Zhengwei Pan. Nature Commun. **11**, 2040 (2020). https://doi.org/10.1038/s41467-020-16015-z
[3] Y. Zhou, D.D. Jia, L.A. Lewis, S.P. Feofilov, R.S. Meltzer. Nucl. Instrum. Meth. A **633**, 31 (2011). https://doi.org/10.1016/j.nima.2010.12.238
[4] B. Caillier, J. Caiut, C. Muja, J. Demoucron, R. Mauricot, J. Dexpert-Ghys, Ph. Guillot. Photochem. Photobiol. **91**, 526 (2015). https://doi.org/10.1111/php.12426
[5] H. Kitagawa, T. Nomura, T. Nazmul, K. Omori, N. Shigemoto, T. Sakaguchi, H. Ohge. Am. J. Infect. Control **49**, 299 (2021). https://doi.org/10.1016/j.ajic.2020.08.022
[6] S. Miwa, S. Yano, Y. Hiroshima, Y. Tome, F. Uehara, S. Mii, E.V. Efimova, H. Kimura, K. Hayashi, H. Tsuchiya, R.M. Hoffman. J. Cell. Biochem. **114**, 2493 (2013). https://doi.org/10.1002/jcb.24599
[7] Puxian Xiong, Mingying Peng. Opt. Mater. X **2**, 100022 (2019). https://doi.org/10.1016/j.omx.2019.100022
[8] G.V. Belessiotis, P.P. Falara, I. Ibrahim, A.G. Kontos. Materials **15**, 4629 (2022). https://doi.org/10.3390/ma15134629
[9] M. Broxtermann, L.M. Funke, J.-N. Keil, H. Eckert, M.R. Hansen, A. Meijerink, T. Yu, N. Braun, Th. Jüstel. J. Lumin. **202**, 450 (2018). https://doi.org/10.1016/j.jlumin.2018.05.056
[10] M. Ferhi, K. Horchani-Naifer, S. Hraiech, M. Ferid, Y. Guyot, G. Boulon. Rad. Meas. **46**, 1033 (2011). http://dx.doi.org/10.1016/j.radmeas.2011.06.062

[11] J.M.A. Caiut, S. Lechevallier, J. Dexpert-Ghys, B. Caillier, Ph. Guillot. J. Lumin. **131**, 628 (2011). https://doi.org/10.1016/j.jlumin.2010.11.004
[12] J. Kappelhoff, J.-N. Keil, M. Kirm, V.N. Makhov, K. Chernenko, S. Moller, Th. Jüstel. Chem. Phys. **562**, 111646 (2022). https://doi.org/10.1016/j.chemphys.2022.111646
[13] L.A. Boatner. Rev. Mineral. Geochem. **48**, 87 (2002). https://doi.org/10.2138/rmg.2002.48.4
[14] M. Ridley, B. McFarland, C. Miller, E. Opila. Materialia **21**, 101289 (2022). https://doi.org/10.1016/j.mtla.2021.101289
[15] A.E. Grechanovsky, N.N. Eremin, V.S. Urusov. FTT **55**, 1813 (2013). (in Russian).
[16] A.G. Herández, D. Boyer, A. Potdevin, G. Chadeyron, A. G. Murillo, F. de J.C. Romo, R. Mahiou. Opt. Mater. **73**, 350 (2017). https://doi.org/10.1016/j.optmat.2017.08.034
[17] V.S. Levushkina, D.A. Spassky, E.M. Aleksanyan, M.G. Brik, M.S. Tretyakova, B.I. Zadneprovski, A.N. Belsky. J. Lumin. **171**, 33 (2016). https://doi.org/10.1016/j.jlumin.2015.10.074
[18] D. Spassky, A.N. Vasil'ev, V. Nagirnyi, I. Kudryavtseva, D. Deyneko, I. Nikiforov, I. Kondratyev, B. Zadneprovski. Materials **15**, 6844 (2022). https://doi.org/10.3390/ma15196844
[19] V.S. Voznyak-Levushkina, A.A. Arapova, D.A. Spassky, I.V. Nikiforov, B.I. Zadneprovsky. FTT **64**, *12*, 1925 (2022). (in Russian). https://doi.org/10.21883/FTT.2022.12.53644.449
[20] T. Lyu, P. Dorenbos. J. Mater. Chem. C **6**, 369 (2018). https://doi.org/10.1039/c7tc05221a
[21] Congting Sun, Dongfeng Xue. Dalton Trans. **46**, 7888 (2017). https://doi.org/10.1039/c7dt01375b
[22] A. Belsky, A. Gektin, A.N. Vasil'ev. Phys. Status Solidi B **257**, 1900535 (2020). http://dx.doi.org/10.1002/pssb.201900535
[23] R. Kirkin, V.V. Mikhailin, A.N. Vasil'ev. IEEE T. Nucl. Sci. **59**, *5*, 2057 (2012). http://dx.doi.org/10.1109/TNS.2012.2194306
[24] A. Trukhin, L.A. Boatner. Mater. Sci. Forum. Trans. Tech. Publications Aedermannsdorf, Switzerland. **239**, 573 (1997).
[25] E. Nakazawa. Chem. Phys. Lett. **56**, 161 (1978). https://doi.org/10.1016/0009-2614(78)80210-3
[26] L. van Pieterson, M. Heeroma, E. de Heer, A. Meijerink. J. Lumin. **91**, 177 (2000). https://doi.org/10.1016/S0022-2313(00)00214-3
[27] M. Nikl, A. Yoshikawa, T. Fukuda. Opt. Mater. **26**, 545 (2004). http://dx.doi.org/10.1016/j.optmat.2004.05.002
[28] D. Krasikov, A. Scherbinin, A. Vasil'ev, I. Kamenskikh, V. Mikhailin. J. Lumin. **128**, 1748 (2008). http://doi.org/10.1016/j.jlumin.2008.04.001
[29] A. Fukabori, V. Chani, K. Kamada, A. Yoshikawa. J. Cryst. Growth **352**, 124 (2012). http://dx.doi.org/10.1016/j.jcrysgro.2012.01.027
[30] M. Nikl, N. Solovieva, J. Pejchal, J.B. Shim, A. Yoshikawa, T. Fukuda, A. Vedda, M. Martini, D.H. Yoon. Appl. Phys. Lett. **84**, 882 (2004). http://dx.doi.org/10.1063/1.1645987
[31] R. Shannon. Acta Cryst. A **32**, 751 (1976). https://doi.org/10.1107/S0567739476001551
[32] L. Vegard. Z. Fur. Phys. **5**, *17*, 17 (1921). https://doi.org/10.1007/BF01349680
[33] P. Dorenbos. J. Phys.: Condens. Matter. **25**, 225501 (2013). https://doi.org/10.1088/0953-8984/25/22/225501
[34] P. Dorenbos. Opt. Mater. **69**, 8 (2017). https://doi.org/10.1016/j.optmat. 2017.03.061
[35] O. Voloshyna, O. Sidletskiy, D. Spassky, Ia. Gerasymov, I. Romet, A. Belsky. Opt. Mater. **76**, 382 (2018). https://doi.org/10.1016/j.optmat.2018.01.003
[36] O. Sidletskiy, A. Gektin, A. Belsky. Phys. Status Solidi A **211**, 2384 (2014). https://doi.org/10.1002/pssa.201431137
[37] D. Spassky, S. Omelkov, H. Mägi, V. Mikhailin, A. Vasil'ev, N. Krutyak, I. Tupitsyna, A. Dubovik, A. Yakubovskaya, A. Belsky. Opt. Mater. **36**, 1660 (2014). https://doi.org/10.1016/j.optmat.2013.12.039
[38] A.V. Gektin, A.N. Belsky, A.N. Vasil'ev. IEEE Trans. Nucl. Sci. **61**, 262 (2013). https://doi.org/10.1109/TNS.2013.2277883
[39] D. Spassky, A. Vasil'ev, S. Vielhauer, O. Sidletskiy, O. Voloshyna, A. Belsky. Opt. Mater. **80**, 247 (2018). https://doi.org/10.1016/j.optmat.2018.05.019
[40] Z. Khadraoui, K. Horchani-Naifer, M. Ferhi, M. Ferid. Chem. Phys. **457**, 37 (2015). http://dx.doi.org/10.1016/j.chemphys.2015.05.014
[41] F. Kang, G. Sun, P. Boutinaud, F. Gao, Z. Wang, J. Lu, S. Xiao. J. Mater. Chem. C **7**, *32*, 9865 (2019). https://doi.org/10.1039/c9tc01385g
[42] L. Han, Ch. Guo, Zh. Ci, Ch. Wang, Yu. Wang, Y. Huang. Chem. Eng. J. **312**, 204 (2017). http://dx.doi.org/10.1016/j.cej.2016.11.136
[43] D.J. Singh, G.E. Jellison, Jr., L.A. Boatner. Phys. Rev. B **74**, 155126 (2006). http://dx.doi.org/10.1103/PhysRevB.74.155126
[44] A.N. Trukhin, L.A. Boatner. In: Proceeding of the 5th Int. Conf. on Inorganic Scintillators and their Applications / Ed. V. Mikhailin. University of Moscow, Russia, M. (2000). P. 697–702.
[45] G. Stryganyuk, S. Zazubovich, A. Voloshinovskii, M. Pidzyrailo, G. Zimmerer, R. Peters, K. Petermann. J. Phys.: Condens. Matter **19**, 036202 (2007). http://dx.doi.org/10.1088/0953-8984/19/3/036202
[46] N.V. Guerassimova, I.A. Kamenskikh, V.V. Mikhailin, I.N. Shpinkov, D.A. Spassky, E.E. Lomonova, M.A. Borik, N.I. Markov, V.A. Panov, M.A. Veshnyakova, M. Kirm, G. Zimmerer. Nucl. Instrum. Meth. A **486**, *1–2*, 234 (2002). http://dx.doi.org/10.1016/S0168-9002(02)00708-8
[47] I.A. Kamenskikh, N. Guerassimova, C. Dujardin, N. Garnier, G. Ledoux, C. Pedrini, M. Kirm, A. Petrosyan, D. Spassky. Opt. Mater. **24**, 267 (2003). http://dx.doi.org/10.1016/S0925-3467(03)00133-2

Translated by E.Ilinskaya